ACOUSTICS 2025
JOONDALUP
SOUNDS OF THE SUNSET COAST

Aspects of a seafloor with fast fluid layer over basement half-space with fast shear speed

Adrian D. Jones

Ocean Acoustics Associates, P.O. Box 333, Blackwood, SA 5051, Australia

ABSTRACT

A seafloor half-space consisting of either a fast, absorbing fluid, or an elastic solid with fast shear speed, may be expected to be nearly totally reflective for plane waves incident at grazing angles less than critical. However, for a seafloor with a fast fluid layer over an elastic basement with fast shear speed, sound incident at angles less than critical may undergo high reflection loss for certain circumstances, as has been shown in prior work. This paper reviews the relevant theory and shows how the two zones of high loss may be identified through considerations of impedance. Some new developments of the analysis are shown. These include a simplification which may be used to more readily identify one of the zones of high loss. Where possible, the new aspects of this analysis are illustrated with reference to prior work.

1 INTRODUCTION

The reflection of plane wave acoustic signals from a seafloor formed with a fluid sediment layer over an elastic basement is a subject for which many aspects have been well studied. Most existing work has been in relation to seafloors for which the basement half-space has a “fast” speed of compressional waves, but has a “slow” shear wave speed. That is, the speed of compressional waves in the basement $c_{p_{ba}}$ exceeds the speed of sound in seawater c_W, but the speed of shear waves in the basement $c_{s_{ba}}$ is less than c_W. As is well known, the consequence is that for all angles of sound incidence β at the layered seafloor, a shear wave will be transmitted into the basement, whereas compressional waves are not transmitted into the basement unless angle β exceeds the critical angle $\beta_{cp_{ba}} = \arccos\left(c_W / c_{p_{ba}}\right)$ for a compressional wave in the basement. Even if the sediment layer has a fast compressional speed $c_{p_{se}}$, and the water-borne sound is incident at angles less than its critical angle $\beta_{c_{se}} = \arccos\left(c_W / c_{p_{se}}\right)$, as well as less than critical angle $\beta_{cp_{ba}}$ for the basement, the layered seafloor may be highly absorbent, that is, exhibit a high bottom loss in dB. A description for this bottom loss for small grazing angles (Jones, 2025), highlighted the progressive reduction in loss caused by increasing the layer thickness. The present paper is a sequel to that earlier work. For ease of understanding, some expressions in the earlier paper are repeated.

For small angles of sound incidence, a seafloor half-space of either a fast, absorbing fluid, or of an elastic solid with fast shear and compressional speeds, may be shown to be nearly totally reflective. However, as has been shown in the literature (Hovem and Kristensen, 1992) (Ainslie, 1999) (Ainslie, 2003), the reflection from the seafloor that consists of a fast fluid layer over a basement with fast shear speed may be profoundly different, especially when the shear speed of the latter, $c_{s_{ba}}$, is considerably greater than c_W. In particular, two zones of high bottom loss may exist. Reflection from this layered seafloor type has received vastly less attention in the literature than that for which the basement has slow shear speed.

The reflection from this seafloor type is illustrated in Figure 1. The compressional wave speeds have relativity $c_{p_{ba}} > c_{p_{se}} > c_W$, and the basement shear speed has relativity $c_{s_{ba}} > c_W$. Relevant incidence angles β at the seawater-sediment boundary are assumed less than the critical angle for compressional waves in the sediment layer, and less than the critical angles for each of compressional and shear waves in the basement. As a result, the angles of compressional waves $\beta_{p_{se}}$ within the sediment, and $\beta_{p_{ba}}$ within the basement, as well as the angle of shear waves in the basement $\beta_{s_{ba}}$, may each be shown to be complex, as indicated in Figure 1. Here, the critical angle for the basement shear speed $\beta_{cs_{ba}} = \arccos\left(c_w / c_{s_{ba}}\right)$. Within the sediment, an evanescent wave propagates horizontally at a speed $c_w / \cos\beta$, less than $c_{p_{se}}$. Within the basement, evanescent waves travel at the same speed.

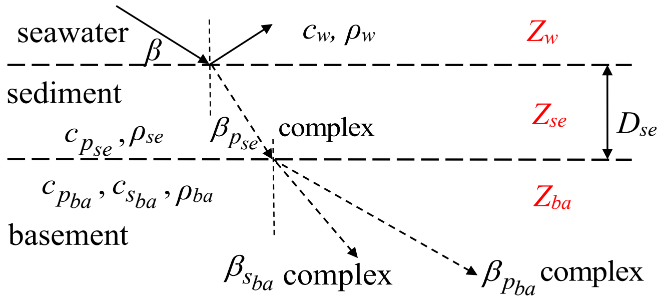

Source (Author, 2025)

Figure 1: Sound incident at fast fluid layer over elastic half-space with fast shear speed, when incident angle β is less than compressional critical angles in sediment and in basement, and less than shear critical angle in basement. Evanescent waves shown by dashed arrow lines.

2 REFLECTION AT LAYERED SEAFLOOR

As is well known, e.g. Brekhovskikh and Godin (Brekhovskikh and Godin, 1998) in their equation (2.4.17), for a seafloor with a uniform fluid layer over a uniform elastic basement, the sound pressure reflection coefficient for an acoustic plane wave at frequency f incident at the seawater/seafloor interface at angle β may be expressed as

$$R\left(\beta, \phi_{se}\right) = \frac{R_{w/se}(\beta) + R_{se/ba}\left(\beta_{p_{se}}\right)\exp\left(2i\phi_{se}\right)}{1 + R_{w/se}(\beta) R_{se/ba}\left(\beta_{p_{se}}\right)\exp\left(2i\phi_{se}\right)}. \tag{1}$$

Here, $R_{w/se}(\beta)$ is the reflection coefficient at angle β at a boundary between seawater and a half-space of fluid layer material, $R_{se/ba}\left(\beta_{p_{se}}\right)$ is the reflection coefficient at a fluid layer-basement boundary at angle $\beta_{p_{se}}$ (related to β by Snell's law), $\phi_{se} \equiv k_{se} D_{se} \sin\beta_{p_{se}}$ is the vertical phase delay for the compressional wave crossing the fluid layer and D_{se} is the thickness of layer, m. As is well-known, these reflection coefficients, in turn, may be expressed in terms of the impedances $Z_w = \dfrac{\rho_w c_w}{\sin\beta}\ \mathrm{kg\,m^{-2}s^{-1}}$, $Z_{se} = \dfrac{\rho_{se} c_{p_{se}}}{\sin\beta_{p_{se}}}\ \mathrm{kg\,m^{-2}s^{-1}}$ and Z_{ba}, of the seawater, layer and basement, respectively, as $R_{w/se}(\beta) = \dfrac{Z_{se} - Z_w}{Z_{se} + Z_w}$ and $R_{se/ba}\left(\beta_{p_{se}}\right) = \dfrac{Z_{ba} - Z_{se}}{Z_{ba} + Z_{se}}$. Making these substitutions, after manipulation, (1) becomes

$$R\left(\beta, \phi_{se}\right) = \frac{Z_{se}\left(Z_{ba} - Z_w\right) - i\left(Z_{se}^2 - Z_w Z_{ba}\right)\tan\phi_{se}}{Z_{se}\left(Z_{ba} + Z_w\right) - i\left(Z_{se}^2 + Z_w Z_{ba}\right)\tan\phi_{se}}. \tag{2}$$

Of course, the overall reflection coefficient $R(\beta,\phi_{se})$ of the layered seafloor in (1) may also be described using its overall normal acoustic impedance Z_{ov} kg/(m^{2}s), as $R(\beta,\phi_{se}) = \frac{Z_{\text{ov}} - Z_w}{Z_{\text{ov}} + Z_w}$, and making this substitution in (2) results in the convenient expression

$$Z_{\text{ov}} = \frac{Z_{se}\left[Z_{ba} - iZ_{se}\tan\phi_{se}\right]}{Z_{se} - iZ_{ba}\tan\phi_{se}} \text{ kg m}^{-2}\text{s}^{-1}. \tag{3}$$

2.1 Reflection at Grazing Incidence, Fast Shear Speed in Elastic Basement

For the layered seafloor type of Figure 1, the wave speeds have relativity $c_{p_{ba}} > c_{p_{se}} > c_w$, and $c_{s_{ba}} > c_w$. It will be assumed that the incidence angle β at the seawater-sediment boundary is less than the critical angle for the sediment layer $\beta_{c_{se}}$, and less than the critical angles $\beta_{cp_{ba}}$ and $\beta_{cs_{ba}}$ for the basement. For these small angles, for the sediment layer $\cos\beta > \cos\beta_{c_{se}}$, that is $\cos\beta > \left(c_w / c_{p_{se}}\right)$, so from Snell's Law, for which $\cos\beta_{p_{se}} = \left(c_{p_{se}} / c_w\right)\cos\beta$, $\cos\beta_{p_{se}} > 1$. From the expression $\sin^2\beta_{p_{se}} = 1 - \cos^2\beta_{p_{se}}$, $\sin^2\beta_{p_{se}}$ is then negative with $\sin^2\beta_{p_{se}} = -\left(\cos^2\beta_{p_{se}} - 1\right)$, giving $\sin\beta_{p_{se}} = i\sqrt{\cos^2\beta_{p_{se}} - 1}$, so that the angle $\beta_{p_{se}}$ is complex. Using the above Snell's Law substitution gives $\sin\beta_{p_{se}} = i\frac{c_{p_{se}}}{c_w}\sqrt{\sin^2\beta_{c_{se}} - \sin^2\beta}$, hence the impedance Z_{se} is purely imaginary, as

$$Z_{se} = -i\frac{\rho_{se}c_w}{\left[\sin^2\beta_{c_{se}} - \sin^2\beta\right]^{\frac{1}{2}}} \text{ kg m}^{-2}\text{s}^{-1}. \tag{4}$$

It also follows that the vertical phase delay for the layer becomes

$$\phi_{se} = i\left|\phi_{se}\right| = iD_{se}k_{p_{se}}\frac{c_{p_{se}}}{c_w}\left[\sin^2\beta_{c_{se}} - \sin^2\beta\right]^{\frac{1}{2}}. \tag{5}$$

Using the general substitution $i\tan(i\,x) = -\tanh x$, with the above ϕ_{se}, in (2) and (3) gives the convenient forms

$$R(\beta,\phi_{se}) = \frac{Z_{se}\left(Z_{ba} + Z_{se}\tanh\left|\phi_{se}\right|\right) - Z_w\left(Z_{se} + Z_{ba}\tanh\left|\phi_{se}\right|\right)}{Z_{se}\left(Z_{ba} + Z_{se}\tanh\left|\phi_{se}\right|\right) + Z_w\left(Z_{se} + Z_{ba}\tanh\left|\phi_{se}\right|\right)} \tag{6}$$

and $$Z_{\text{ov}} = \frac{Z_{se}\left[Z_{ba} + Z_{se}\tanh\left|\phi_{se}\right|\right]}{Z_{se} + Z_{ba}\tanh\left|\phi_{se}\right|} \text{ kg m}^{-2}\text{s}^{-1}. \tag{7}$$

Equations (6) and (7) were derived in the previous paper (Jones, 2024) for a basement with a slow shear speed, but are equally applicable to the present case with a fast shear speed for the basement. For the present case, the angle of shear waves in the basement $\beta_{s_{ba}}$ is complex, so the expressions for components of the basement impedance derived in the previous paper, Equations (13) and (14) of Jones (Jones, 2024), must be modified accordingly. The basement impedance Z_{ba} now becomes

$$Z_{ba} = 4i\,\rho_{ba} c_w \left(\frac{c_{s_{ba}}}{c_w}\right)^4 \cos^2\beta \sqrt{\sin^2\beta_{cs_{ba}} - \sin^2\beta} \; - \; \frac{i\,\rho_{ba} c_w \left[1 - 2\left(\frac{c_{s_{ba}}}{c_w}\cos\beta\right)^2\right]^2}{\sqrt{\sin^2\beta_{cp_{ba}} - \sin^2\beta}} \text{ kg m}^{-2}\text{s}^{-1}. \tag{8}$$

In general, impedances may have real and imaginary parts, so strictly, $Z_{se} = X_{se} + iY_{se}$ and $Z_{ba} = X_{ba} + iY_{ba}$. In the above expressions (4) and (8) for impedances Z_{se} and Z_{ba}, respectively, the real parts are each zero. This differs from the case for which the basement has a slow shear speed (Jones, 2024) in that Z_{ba} then had a real component, as well as an imaginary component. The fact that both components of the impedance Z_{ba} in (8) are imaginary has a profound effect, as shown later.

3 CONDITIONS FOR HIGH LOSS

From the expression for reflection coefficient $R(\beta,\phi_{se}) = (Z_{\text{ov}} - Z_w)/(Z_{\text{ov}} + Z_w)$ given earlier, it is obvious that for any seafloor, layered or not, $R(\beta,\phi_{se}) = 0$ corresponds with $Z_{\text{ov}} = Z_w \text{ kg m}^{-2}\text{s}^{-1}$. Making this substitution in (7) gives, for total loss, $Z_w = \dfrac{Z_{se}\left[Z_{ba} + Z_{se}\tanh|\phi_{se}|\right]}{Z_{se} + Z_{ba}\tanh|\phi_{se}|} \text{ kg m}^{-2}\text{s}^{-1}$, from which it follows that

$$\tanh|\phi_{se}| = \frac{Z_{se}\left(Z_w - Z_{ba}\right)}{\left[Z_{se}^{\;2} - Z_w Z_{ba}\right]}. \tag{9}$$

As seawater impedance $Z_w = \dfrac{\rho_w c_w}{\sin\beta} \text{ kg m}^{-2}\text{s}^{-1}$, it immediately follows that one solution for total loss occurs when $\sin\beta \approx \beta \to 0^+$, resulting in $\tanh\left|\phi_{se_0}\right| = -\dfrac{Z_{se_0}}{Z_{ba_0}} = -\dfrac{Y_{se_0}}{Y_{ba_0}}$, where the subscript "0" implies the value of the quantity for incident grazing angle $\beta \to 0^+$. In general, $\tanh|x|$ must be real and between 0 and 1, so the same applies to $\tanh|\phi_{se}|$. This requires that Z_{ba_0} is positive imaginary, as from (4) $Z_{se_0} \approx -i\dfrac{\rho_{se} c_w}{\sin\beta_{c_{se}}} \text{ kg m}^{-2}\text{s}^{-1}$ is *always* negative imaginary. From (8), Z_{ba_0} follows as

$$Z_{ba_0} \approx 4i\,\rho_{ba} c_w \left(\frac{c_{s_{ba}}}{c_w}\right)^4 \sin\beta_{cs_{ba}} \; - \; i\frac{\rho_{ba} c_w}{\sin\beta_{cp_{ba}}}\left[1 - 2\left(\frac{c_{s_{ba}}}{c_w}\right)^2\right]^2 \text{ kg m}^{-2}\text{s}^{-1}. \tag{10}$$

Making the reasonable assumptions, that for the elastic basement with relatively high shear speed, this shear speed $c_{s_{ba}}$ is half the basement compressional speed $c_{p_{ba}}$, that $c_w = 1500 \text{ m/s}$ and that $\rho_{ba} \approx 2600 \text{ kg}\cdot\text{m}^{-3}$, it may be shown from (10) that Z_{ba_0} will be positive imaginary if $c_{s_{ba}}$ is greater than about 1610 m/s. However, to ensure that $0 < \tanh|\phi_{se}| \le 1$ in (9), the impedances must be such that $Z_{ba_0} > -Z_{se_0}$, that is $Y_{ba_0} > -Y_{se_0}$. From (4) this requires $Y_{ba_0} > \dfrac{\rho_{se} c_w}{\sin\beta_{c_{se}}} \text{ kg m}^{-2}\text{s}^{-1}$, giving the requirement

$$c_{p_{se}} > \frac{c_w}{\sqrt{1-\left(\rho_{se}c_w/Y_{ba_0}\right)^2}}. \tag{11}$$

A second solution to (9), giving total loss, occurs when $Z_{ba} \to -Z_{se}$, giving $\tanh\left|\phi_{se}\right| \to 1$. The two scenarios for which total loss occurs, with $R\left(\beta,\phi_{se}\right)=0$, have now been obtained. As is shown, absorption within the sediment and basement modify the second solution significantly. Note that each of these two solutions may also be obtained from (6) by setting the numerator to zero, to correspond with $R\left(\beta,\phi_{se}\right)=0$.

3.1 Resonance of Evanescent Wave

From the general form for the hyperbolic tangent, $\tanh x = \left(e^x - e^{-x}\right)/\left(e^x + e^{-x}\right)$, hence (9) may be written as

$$\exp\left(2\left|\phi_{se}\right|\right) = \left[\frac{Z_w + Z_{se}}{Z_w - Z_{se}}\right]\left[\frac{Z_{ba} - Z_{se}}{Z_{ba} + Z_{se}}\right]. \tag{12}$$

Assuming that incident grazing angle $\beta \to 0^+$, as $Z_w = \dfrac{\rho_w c_w}{\sin\beta}$ kg m^{-2}s^{-1} the first term on the RHS approaches 1. From (5), $\left|\phi_{se_0}\right| \approx k_{p_{se}} D_{se} \tan\beta_{c_{se}}$, so that (12) becomes $\exp\left(2k_{p_{se}} D_{se} \tan\beta_{c_{se}}\right) \approx \left[\dfrac{Z_{ba_0} - Z_{se_0}}{Z_{ba_0} + Z_{se_0}}\right]$. Now, taking logarithms and re-arranging gives the occurrence of total loss occurring for $\beta \to 0^+$ at a value of dimensionless frequency $K = \omega D_{se}/c_{p_{se}}$, written here as K_E and given as follows:

$$K_E\Big|_{\beta\to 0^+} \approx \frac{\cot\beta_{c_{se}}}{2}\ln\left[\frac{Z_{ba_0} - Z_{se_0}}{Z_{ba_0} + Z_{se_0}}\right] \text{ non-dimensional.} \tag{13}$$

This is the same as Ainsley's equation (8) (Ainslie, 2003) in which the term ζ_0 was used to represent the impedance ratio Z_{ba_0}/Z_{se_0}. Ainslie (Ainslie, 2003) refers to this occurrence of total loss as a resonance of the evanescent wave. At resonance, it is simple to show that the thickness of the sediment layer is $K_E/(2\pi)$ wavelengths, and $\tanh\left|\phi_{se_0}\right| \approx \tanh\left[K_E \tan\beta_{c_{se}}\right]$. Although not shown here for sake of brevity, the inclusion of absorption within the sediment layer moves the zone of highest loss to a small positive grazing angle β. For most practical seafloor examples, the consequence of this type of loss is limited, as its occurrence is confined to very small angles of sound incidence.

3.2 Speed of Sholte Wave at Surface of Elastic Basement

As discussed by Ainslie (Ainslie, 2003), a Scholte wave is a wave at the surface of an elastic solid, at which an interface exists with a liquid. (Previously, Ainslie in his earlier paper (Ainslie, 1999), and Hovem and Kristensen (Hovem and Kristensen, 1992), each referred to this surface wave as a Stoneley wave.) It is simple to show that the speed of a Scholte wave corresponds with that of the evanescent wave in the sediment layer, when the angle of sound incidence at the layered seafloor, being less than critical, causes the value of Z_{ba} from (8) to be equal to $-Z_{se}$ obtained using (4). By inference, the second type of total loss, for which $Z_{ba} \to -Z_{se}$, must be related to the excitation of the Sholte wave at the surface of the elastic basement.

Assuming that, the grazing angle β_{Sch} is that which corresponds with the speed of the evanescent wave in the sediment being the same as the speed of the Scholte wave c_{Sch}, giving $c_{Sch} = c_w / \cos\beta_{Sch}$. Making the substitution β_{Sch} for β in the impedance expressions (4) and (8), then equating Z_{se} with $-Z_{ba}$ for this angle, gives

$$-\left[2-\left(\frac{c_{Sch}}{c_{s_{ba}}}\right)^2\right]^2+4\left[1-\left(\frac{c_{Sch}}{c_{s_{ba}}}\right)^2\right]^{\frac{1}{2}}\left[1-\left(\frac{c_{Sch}}{c_{p_{ba}}}\right)^2\right]^{\frac{1}{2}}-\frac{\rho_{se}}{\rho_{ba}}\left(\frac{c_{Sch}}{c_{s_{ba}}}\right)^4\left[1-\left(\frac{c_{Sch}}{c_{p_{ba}}}\right)^2\right]^{\frac{1}{2}}\left[1-\left(\frac{c_{Sch}}{c_{p_{se}}}\right)^2\right]^{-\frac{1}{2}}=0. \qquad (14)$$

Equation (14) is identical to equation (2.98) of Tolstoy and Clay (Tolstoy and Clay, 1987), this expression being referenced by Ainslie as giving the speed of a Scholte wave.

3.3 Excitation of Scholte Wave

The second scenario for which total loss exists for the layered seafloor was identified as occurring when $Z_{ba}\to -Z_{se}$ (same as $Y_{ba}\to -Y_{se}$). Of course, if this is substituted in (12), the result is for $|\phi_{se}|$ to approach infinity. However, this is no longer the result when absorptions within the sediment and basement are included in (12), as real parts X_{se} and X_{ba}, respectively, of the impedances Z_{se} and Z_{ba}, whilst retaining the assumption $Y_{ba}\to -Y_{se}$. After manipulation and approximation, (12) now becomes

$$\exp\left(2\left|\phi_{se_S}\right|\right)\approx\left[\frac{Z_{w_S}+Z_{se_S}}{Z_{w_S}-Z_{se_S}}\right]\left[\frac{2iY_{ba_S}}{X_{ba_S}+X_{se_S}}\right] \qquad (15)$$

where the subscript “S” implies evaluation at the Scholte angle, β_{Sch}.

Further evaluation to determine the relevant values of $|\phi_{se}|$ requires consideration of the first term on the RHS of (15). Hovem and Kristensen (Hovem and Kristensen, 1992) make the assumption that a simplification of this term may be obtained by assuming that the relevant grazing angle approaches $\beta_{c_{se}}$, the critical angle in the sediment. From (4), Z_{se} then becomes very large, so the first term on the RHS of (15) may be approximated as -1. This assumption is mathematically awkward, as it results in taking the exponential of a negative imaginary value. Further, if the grazing angle actually approaches $\beta_{c_{se}}$, some infeasible results follow. For example, from (5), ϕ_{se} should approach zero. A pragmatic approach used in this paper is to evaluate the first term on the RHS of (15) for the grazing angle β for which $|Z_w|=|Y_{se}|$, as $Z_w=i\left(iY_{p_{se}}\right)=iZ_{se}$. As $Z_w=\frac{\rho_w c_w}{\sin\beta}\ \mathrm{kg\,m^{-2}s^{-1}}$, from (4) the sine of this angle may be shown to be

$$\sin\beta=\frac{\sin\beta_{c_{se}}}{\sqrt{\left[\left(\rho_{se}/\rho_w\right)^2+1\right]}}, \qquad (16)$$

hence this angle β is clearly less than $\beta_{c_{se}}$. Substituting $Z_w=iZ_{se}$, the first term on the RHS of (15) then becomes $-i$, and the complete RHS becomes totally real, as $\exp\left(2\left|\phi_{se_S}\right|\right)\approx\left[\frac{2Y_{ba_S}}{X_{ba_S}+X_{se_S}}\right]$. After taking logarithms of each side, and substituting from (5), the value of $K=\omega D_{se}/c_{p_{se}}$ for maximum loss is

$$K_S \approx \frac{c_w}{2c_{p_{se}}\left[\sin^2\beta_{c_{se}} - \sin^2\beta_{Sch}\right]^{\frac{1}{2}}} \ln\left[\frac{2Y_{ba_S}}{X_{ba_S} + X_{se_S}}\right] \text{ non dimensional.} \tag{17}$$

In practice, the value of absorption within the basement is small and X_{ba_S} may be deleted. Following a similar derivation as Chapman (Chapman, 2001) used to obtain his equation (1.8a), but for finite angles of incidence β, it may be shown that

$$X_{se}(\beta) \approx \frac{\rho_{se} c_w \alpha_{p_{se}} \cos^2\beta_{c_{se}}}{40\pi \log(e)\left[\sin^2\beta_{c_{se}} - \sin^2\beta\right]^{\frac{3}{2}}} \text{ kg m}^{-2}\text{s}^{-1} \tag{18}$$

where $\alpha_{p_{se}}$ is the absorption of compressional waves in the sediment layer dB/λ, hence X_{se_S} may be determined once the Scholte angle β_{Sch} is known.

Equation (17) is more convenient for application than Ainslie's equation 20 (Ainslie, 2003) which is in terms of the speed of the Scholte wave. Equation (17) does, however, require a value for the Scholte angle β_{Sch}. (Of course, that angle, itself, is linked to the speed of the Scholte wave, as $c_{Sch} = c_w / \cos\beta_{Sch}$.) As more convenient than first obtaining the Scholte wave speed from (14), a pragmatic approach was taken to estimate β_{Sch}. Here, it was observed that, for typical sets of geoacoustic parameters, the decline in amplitude of Z_{ba} from Z_{ba_0} (using (8)), with increasing grazing angle β, was approximately matched to the rise in amplitude of Z_{se} from Z_{se_0} (using (4)). For example, from (4)

$$Z_{se} \approx Z_{se_0} + Z_{se_0}\frac{\sin^2\beta}{2\sin^2\beta_{c_{se}}} \text{ kg m}^{-2}\text{s}^{-1} \text{ for } \beta \ll \beta_{c_{se}}. \tag{19}$$

The corresponding expression for Z_{ba} may be shown to be similar, approximately, with a decline of similar amplitude in proportion to $\sin^2\beta$. Very approximately, at the grazing angle at which $|Y_{ba}| \approx |Y_{se}|$, each of $|Y_{ba}|$ and $|Y_{se}|$ is then about the average of $|Y_{ba_0}|$ and $|Y_{se_0}|$. Thus, the estimate for $|Y_{ba_S}| = |Y_{se_S}|$ at the Sholte angle was obtained by averaging the values existing at zero grazing angle, as $|Y_{ba_S}| = |Y_{se_S}| = \frac{1}{2}\left(|Y_{ba_0}| + |Y_{se_0}|\right)$. The grazing angle β_{Sch} was then estimated as that at which $|Y_{se_S}|$ from (4) is equal to $\frac{1}{2}\left(|Y_{ba_0}| + |Y_{se_0}|\right)$. This angle follows as

$$\sin\beta_{Sch} \approx \sin\beta_{c_{se}}\left[1 - \frac{Y_{se_0}{}^2}{Y_{se_S}{}^2}\right]^{1/2}. \tag{20}$$

As shown in Section 4, this appears to be an effective approximation. Lastly, it may be noted that occurrence of the high bottom loss associated with (17) is not solely due to the evanescent wave in the sediment layer travelling at the Scholte wave speed, as this may occur for any acoustic frequency. Since (17) indicates a particular frequency-layer thickness combination, it may be assumed that this loss event is associated with a resonance of the evanescent wave involving the Scholte wave. For practical seafloor examples, as this zone of high loss occurs for incidence angles between zero and the layer critical angle $\beta_{c_{se}}$, it may cause a significant reduction in the acoustic transmission in a shallow ocean, for which loss at small angles is detrimental.

3.4 Geoacoustic Parameters Permitting Loss

In Section 3, a requirement for the first loss mechanism that ensures $Y_{ba_0} > -Y_{se_0}$, that is $Y_{ba_0} > \left|Y_{se_0}\right|$, was shown to be given by (11). This sets a limit for the minimum value of sediment sound speed $c_{p_{se}}$ to permit the resonance of the evanescent wave. Some initial estimates will now be made for this value.

Now, for different sediment types, particular relationships may be presumed to exist between density ρ_{se} and sound speed $c_{p_{se}}$. However, for present simplicity, a sediment density of 1700 kg/m^3 will be presumed. To now estimate sets of geoacoustic parameters which would be supportive of the first type of loss mechanism, it will be assumed that for the high basement shear speeds involved, the basement shear speed $c_{s_{ba}}$ is half the basement compressional speed $c_{p_{ba}}$, and basement density is 2600 kg/m^3. Seawater sound speed is estimated as 1500 m/s, seawater density as 1000 kg/m^3. For numeric convenience, the related values of Y_{ba_0} obtained from (10), and designated "nd", are shown in Table 1 as non-dimensionalised with reference to the value of $\rho_w c_w$ for seawater. The resulting requirement for compressional speed in the sediment given by (11) is indicated in the Table, for various values of basement shear speed. From the table, it follows that, for a basement with a shear speed exceeding about 2000 m/s, the requirement for sediment compressional speed will be satisfied for many sediment types. However, for basements of shear speed about 1900 m/s and less, it is less likely that the sediment compressional speed will be sufficient to support the resonance. For basement shear speed 1800 m/s and less, the requirement for sediment compressional speed $c_{p_{se}}$ from (11) becomes infeasibly large.

In the case of the resonance involving the excitation of the Scholte wave, the situation is more complex. Here it is assumed that $Y_{ba_S} \to -Y_{se_S}$, that is $\left|Y_{ba_S}\right| / \left|Y_{se_S}\right|$ approaches 1.0 at the Scholte angle. It may be shown from (4) and (10) that for such a seafloor, the corresponding value $\left|Y_{ba_0}\right| / \left|Y_{se_0}\right|$ at grazing incidence will exceed 1.0 by a material difference. The values of $c_{p_{se}}$ obtained for Table 1, of course, assumed that $\left|Y_{ba_0}\right| / \left|Y_{se_0}\right|$ exceeds 1.0 at grazing incidence by an infinitesimal value. Considering the origin of the inequality (11), the effect for $\left|Y_{ba_0}\right| / \left|Y_{se_0}\right|$ to be materially greater than 1.0 is that an even larger value of $c_{p_{se}}$, than that obtained using (11) and shown in Table 1, is required for the layered seafloor to support the excitation of the Scholte wave.

Table 1: Geoacoustic parameters for resonance of evanescent wave in sediment layer, sound incidence at 0.0°, $c_{p_{ba}} / c_{s_{ba}} = 2$, $c_w = 1500$ m/s, $\rho_w = 1000$ kg/m^3, $\rho_{se} = 1700$ kg/m^3, Y_{ba_0} nd from (10).

shear speed $c_{s_{ba}}$ (m/s)	comp. speed $c_{p_{ba}}$ (m/s)	impedance Y_{ba_0} nd	impedance $\left|Y_{se_0}\right|$ nd	$c_{p_{se}}$ (m/s) required for resonance
1700	3400	0.95	-	infeasibly large
1800	3600	1.80	-	infeasibly large
1900	3800	2.6	< 2.6	>1983m/s
2000	4000	3.4	< 3.4	>1732m/s
2100	4200	4.3	< 4.3	>1633m/s
2200	4400	5.1	< 5.1	>1591m/s
2300	4600	5.9	< 5.9	>1566m/s
2400	4800	6.7	< 6.7	>1551m/s
2500	5000	7.6	< 7.6	>1539m/s

4 VALIDATION AGAINST PRIOR WORK

It is worthy to check elements of this analysis, initially by reference to the example of the sand layer over a basalt basement as considered by Ainslie (Ainslie, 2003) in his Table 1. The geoacoustic parameters used by Ainslie are shown below in Table 2.

Table 2: Geoacoustic properties: layered seafloor, Ainslie's table 1 (Ainslie, 2003).

layer	density (kg/m³)	comp. speed (m/s)	shear speed (m/s)	comp. attn. (dB/λ)	shear attn. (dB/λ)
seawater	1025	1538	-	0.0	-
sand	2035	1788	0.0	0.868	0.0
basalt	2600	4929	2462	0.10	0.20

From the data in Table 2, the values for the critical angles are as follows: $\beta_{c_{se}} = 30.6633°$, $\beta_{cp_{ba}} = 71.8183°$ and $\beta_{cs_{ba}} = 51.3402°$. The values for the impedance components determined at grazing angle $\beta \to 0^+$ are as follows: from (4) $Y_{se_0} = -3.8929$; from (10) $Y_{ba_0} = 6.5954$. Here, the values are normalized with reference to the value of $\rho_w\, c_w$ determined from Table 2. From Ainslie (Ainslie, 2003), the value K_E associated with the frequency of the resonance of the evanescent wave near grazing incidence is 1.14, while using the above values of Y_{se_0} and Y_{ba_0} in (13) gives the near identical value $K_E = 1.1436$. From the approximation of (20), having assumed $\left|Y_{se_S}\right| = \frac{1}{2}\left(\left|Y_{ba_0}\right| + \left|Y_{se_0}\right|\right)$, the estimate of the angle β_{Sch} corresponding with the excitation of the Scholte wave follows as 20.0°. This compares well with the value 22° obtained by Ainslie (Ainslie, 2003). Using this estimated value $\beta_{Sch} = 20.0°$ in (18) gives the corresponding value of $X_{se_S} = 0.431$, and of course Y_{ba_S} is estimated as $\frac{1}{2}\left(\left|Y_{ba_0}\right| + \left|Y_{se_0}\right|\right) = 5.244$. In (17), as the attenuation in the basement is assumed zero ($X_{ba_S} = 0$), the value K_S is then estimated as 3.63. This compares very well with the value 3.71 obtained by Ainslie using his equation 20. The present analysis may then be seen to provide a very good estimate of the grazing angle of high loss β_{Sch} associated with the excitation of the Scholte wave, and the corresponding value of K_S, thus identifying the frequency of occurrence of this zone of high loss. For a thickness of 1 m for the sand layer, for example, the loss due to the Scholte wave excitation then occurs at a frequency around $f = K\, c_{p_{se}} / (2\pi D)$ Hz, and as $K_S = 3.63$, this is near the frequency 1,030 Hz. As $K_E = 1.1436$, the loss due to the resonance of the evanescent wave, near grazing incidence, occurs at around 330 Hz.

The data in Table 2 are similar to those of the layered seafloor example studied by Hovem and Kristensen (Hovem and Kristensen, 1992). These cases include a layer for which the critical angle $\beta_{c_{se}}$ is relatively large, and a basement for which the Scholte angle is well separated from both that critical angle and grazing incidence. Ainslie (Ainslie, 2003) also considers several cases for which the Scholte angle is much smaller. As shown by Ainslie, this results in zones of high loss associated with each of the resonance of the evanescent wave, and the Scholte wave excitation, forming one continuous zone of high loss, extending from grazing incidence to slightly beyond the Scholte angle. One such example, Ainslie's figure 6(b), has a layer of medium silt of 63% porosity over a basement of medium basalt: the geoacoustic parameters are shown in Table 3.

Table 3: Geoacoustic properties: layered seafloor, Ainslie's figure 6(b) (Ainslie, 2003).

layer	density (kg/m³)	comp. speed (m/s)	shear speed (m/s)	comp. attn. (dB/λ)	shear attn. (dB/λ)
seawater	1025	1537.9	-	0.0	-
medium silt 63% porosity	1637	1580.3	0.0	0.38	0.0
medium basalt	2700	5311	2690	0.1	0.2

From the data in Table 3, the critical angle for the medium silt layer $\beta_{c_{se}} = 13.304°$, and the impedance components at grazing angle $\beta \to 0^+$ are, from (4) $Y_{se_0} = -6.939$, and from (10) $Y_{ba_0} = 8.8048$. These values are normalized with reference to the value $\rho_w\, c_w$ determined from Table 3. From Ainslie (Ainslie, 2003), $K_E = 4.28$, whereas from (13), using the above values of Y_{se_0} and Y_{ba_0} gives $K_E = 4.51$. From the approximation of (20), the estimate of the Scholte angle β_{Sch} follows as 6.24°. This compares well with the value of around 7° to 8° observable from Ainslie's figure 6(b) (Ainslie, 2003). Using the estimated $\beta_{Sch} = 6.24°$ in (18) gives

$X_{se_S} = 1.2619$. Of course, Y_{ba_S} is assumed equal to $\frac{1}{2}\left(\left|Y_{ba_0}\right| + \left|Y_{se_0}\right|\right) = 7.8719$, so from (17) K_S is estimated as 6.05. This compares well with the value 6.4 interpreted from Ainslie's figure 6(b).

There is uncertainty that Table 3 replicates the geoacoustic parameters used by Ainslie for his figure 6(b). In a personal communication (Ainslie, 2025), Ainslie confirms that the parameters in Table 3 conform with his intention that they were derived in accord with the techniques of his Appendix A (Ainslie, 2003), and that the resultant value for K_E must be 4.511, not 4.28. The geoacoustic parameters used for Ainslie's figure 6(b) are thus presumed to be slightly different from values in Table 3.

5 CONCLUSIONS

The analysis for reflection of plane acoustic waves from a seafloor with an absorbing fluid layer over an elastic basement with fast shear speed has been re-visited by using a different description of the impedance of the layered seafloor, in particular, one incorporating the hyperbolic tangent of the vertical phase delay across the layer. This provides an alternative identification of the two sets of conditions causing a high bottom loss with this type of seafloor. In addition, a reasonable approximation has been made by which the incidence angle corresponding with the excitation of the Scholte wave may be estimated. This enables the frequency of occurrence of the high loss corresponding with the excitation of the Scholte wave to be well estimated without the need to explicitly determine the speed of the Scholte wave. By comparison with the pre-existing technique, both the Scholte angle and the frequency of occurrence of high loss from the excitation of the Scholte wave appear to be well estimated by the new method.

The first loss mechanism, the resonance of the evanescent wave in the sediment at angles near grazing incidence, is not expected to greatly affect sound transmission. The second loss mechanism, the loss due to the excitation of the Scholte wave at the surface of the elastic basement, may have an effect on both the ambient noise plus long-range sound transmission. In particular, if the Scholte angle is of the order of about 10° or less, the effects of both types of loss may merge, so that at the frequency involved, a zone of high loss may persist for most angles of incidence relevant to transmission in shallow water. When the Scholte wave is excited, the acoustic energy is, mainly, lost to absorption within the sediment layer, but also may be lost to absorption within the basement, if attenuation within the basement is significant.

ACKNOWLEDGEMENT

The author acknowledges the assistance provided by Dr. Michael Ainslie in the identification of the input data used for his 2003 paper.

REFERENCES

Ainslie, M. A. 1999. 'Interface waves in a thin sediment layer: Review and conditions for high loss', *Proc. I.O.A.*, Vol. 2, Part 9: 33-47.
Ainslie, M. A. 2003. 'Conditions for the Excitation of Interface Waves in a Thin Unconsolidated Sediment Layer', *Journal of Sound and Vibration*, Vol. 268: 249–267.
Ainslie, M. A. 2025. Email to Adrian Jones 29th April 2025.
Brekhovskikh, L.M. and Godin, O. A. (1998). *Acoustics of Layered Media I.* 2nd ed., updated printing, Springer-Verlag.
Chapman, D. M. F. 2001. 'What Are We Inverting For?', In: Taroudakis M.I., Makrakis G.N. (eds) *Inverse Problems in Underwater Acoustics*, Springer, New York, NY.
Hovem, J. M. and Kristensen, A. 1992. 'Reflection loss at a bottom with a fluid sediment layer over a hard solid half-space', *J. Acoust. Soc. Am.*, vol. 92, No. 1: 335-340.
Jones, Adrian D. 2024. 'Weston α Description of Seafloor with Fast Fluid Layer over Basement Half-space'. In *Proceedings of Acoustics 2024*, 6-8 November, Gold Coast, Australia.
Tolstoy, I., and Clay, C. S. 1987. *Ocean Acoustics: Theory and Experiment in Underwater Sound*, American Institute of Physics.